RSC Advances

ROYAL SOCIETY OF CHEMISTRY

www.rsc.org/advances

Journal Name

RSCPublishing

ARTICLE

Electrochemical Proton Reduction Catalysed by Selenolato-Manganese Carbonyl Complexes

Cite this: DOI: 10.1039/x0xx00000x

Kaipeng Hou,[a] Sherman J. L. Lauw,[b] Richard D. Webster[b] and Wai Yip Fan *[a]

Received 00th January 2012,
Accepted 00th January 2012

DOI: 10.1039/x0xx00000x

www.rsc.org/

Four manganese selenolato carbonyl complexes $[Mn(CO)_4(\mu\text{-}SePh)]_2$ **1**, $Mn_2(CO)_4(\mu\text{-}CO)(\mu\text{-}SePh)_2(PBu_3)_2$ (**2**, PBu_3=Tri-n-butylphosphine), $Mn(CO)_4(\mu\text{-}SePh)_2Mn(CO)_3(Py)$(**3**, Py=pyridine) and $Mn(CO)_3(SePh)(DPPP)$ (**4**, DPPP=1,3-bis(diphenylphosphino)propane) have been synthesized and structurally characterized by X-ray crystallography. Their electrocatalytic proton reduction properties have been measured with cyclic voltammetry in dichloromethane using CF_3COOH as the proton source. Overpotentials ranging from 0.79V to 0.89V were determined for these complexes. The presence of different ligands such as phosphine and pyridine only made moderate differences on the overpotential and efficiency of the proton reduction process. The first step in the proton reduction pathway occurs via electroreduction of the Mn complexes based on reactivity studies and cyclic voltammetry data.

Introduction

Hydrogen as a clean and renewable fuel has attracted great interest as a replacement for fossil fuels.[1-4] In nature, [NiFe] and [FeFe] hydrogenase enzymes catalyze the reversible proton reduction to molecular hydrogen at low overpotentials and high efficiency.[5] In the [FeFe] hydrogenase, the two iron centres bearing CO and CN ligands are bridged by a unique azadithiolate ligand for which the N atom serves as the site for protonation. In the active site of [NiFe] hydrogenase, the nickel and iron are bridged together by two cysteine residues. The iron centre is also coordinated to two terminal CN^- and one CO ligands while the nickel center is coordinated to two cysteine residues. However, one of the cysteine residues is replaced by selenocysteine in *Dm. baculatum*.[6] The enzymes with the selenocysteine residue appear to exhibit higher proton reduction activities than [NiFe] hydrogenases (Scheme 1 (a), (b)).[7]

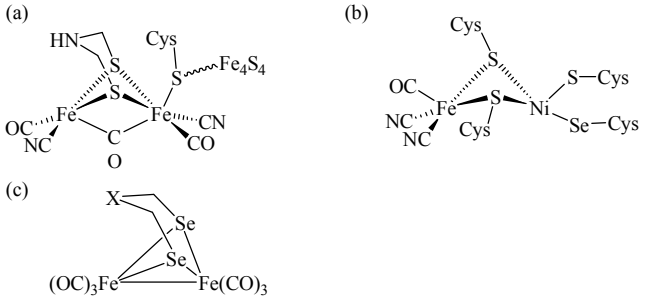

Scheme 1. (a) Active site of [FeFe] hydrogenase (b) Active site of *Dm. baculatum* [NiFeSe] hydrogenase (c)Diiron diselenolato model complexes, X=CH_2, NPh, Se.

Most synthetic models for hydrogenases have been based on Fe/Ni and Fe/Fe thiolato complexes.[8-10] Recently, the syntheses and characterization of diiron diselenolato complexes have been reported (Scheme 1(c)).[14,15] Several structural models of the Ni centre in [NiFeSe] hydrogenases with key features of the Ni site in the H_2 cycling enzyme have also been developed.[16]

In our laboratory, we have recently prepared manganese thiolato carbonyl complexes as [FeFe] hydrogenase models as Mn is also capable of exhibiting multiple oxidation states useful for redox reactions.[17,18] Indeed moderate overpotentials and high TOF have been achieved for some of these Mn complexes. In this work, selenolato ligands have been used for binding to manganese carbonyls instead. We report the syntheses and spectroscopic characterization of a few selenolato dinuclear and monomanganese carbonyl complexes carrying phosphine or pyridine ligands. Their electrocatalytic efficiencies for proton reduction using trifluoroacetic acid CF_3COOH as the proton source in CH_2Cl_2 are evaluated as well.

Results and discussion

Syntheses and Characterization of the Mn Complexes.

The known complex $Mn_2(CO)_8(\mu\text{-}SePh)_2$ **1** as shown in Scheme 2 was prepared by uv irradiation of dimanganese decacarbonyl $Mn_2(CO)_{10}$ in the presence of diphenyl diselenide PhSe-SePh in hexane.[19] Further photolysis of compound **1** with two equivalents of tri-n-butylphosphine PBu_3 in hexane resulted in

complex **2** with a bridged CO ligand: $Mn_2(CO)_4(\mu\text{-}CO)(\mu\text{-}SePh)_2(PBu_3)_2$. The red shift observed for the μ-CO bands of complex **2** compared to **1** in the FTIR spectra is due to the strong electron-donating effect of the phosphine ligands. In addition, a band at 1792 cm^{-1} is observed which was duly assigned to the μ-CO bond of **2**.

The uv photolysis of a one-pot reaction containing $Mn_2(CO)_{10}$, pyridine Py and PhSe-SePh gave **3**, a dimanganese complex of formula $Mn(CO)_4(\mu\text{-}SePh)_2Mn(CO)_3(Py)$. This complex is structurally similar to **1** except that one of the CO ligands has been replaced by pyridine. A one-pot uv irradiation of $Mn_2(CO)_{10}$, 1,3-bis(diphenylphosphino)propane (DPPP) and PhSe-SePh yielded a monomanganese complex **4,** $Mn(CO)_3(SePh)(DPPP)$. Three □CO bands were observed for this complex at 1904(s), 1945(s) and 2010(vs). When excess amount of CF_3COOH was added to the solution of **4** in CH_2Cl_2, no immediate IR change is observed. However, after an hour, three new CO bands appeared at slightly blue-shifted values of 1918(s), 1967(s), 2035(vs) as compared to **4**. This complex **5** of formula $Mn(CO)_3(CF_3COO)(DPPP)$ was obtained upon displacement of the selenolato group of **4** by the CF_3COO^- group. All the complexes have been characterized by IR, ^1H NMR, and X-ray crystallographic methods. Suitable crystals of **2**, **3**, **4** and **5** were grown by dissolving them in a dichloromethane/hexane mixture and stored at low temperatures. Good quality crystals were subjected to X-ray diffraction studies with the structures shown in Figures 1-4.

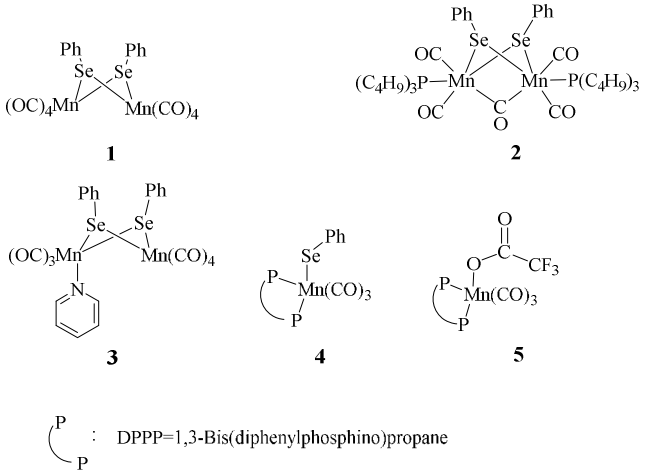

Scheme 2. Structures of complexes **1** to **5**.

X-ray crystal structure

Figure 1 shows the X-ray structure of complex **2** for which a distorted octahedral geometry is observed for each Mn center, bridged by a CO ligand and two μ-selenolato ligands. The distance between the manganese center and carbon in the bridging CO is 2.032(3)Å (Mn1-C13), which is longer than that of the Mn-terminal CO bond (1.795Å, Mn1-C15). The distance between the two Mn centers is 2.6528(6)Å.The phosphorus and manganese atoms lie in a zigzag orientation with P2-Mn2-Mn1 and Mn2-Mn1-P1 angles of 144.19(3)° and 144.52(3) ° respectively. The Mn_2Se_2 ring is not planar as the internal angles do not add up to 360°.

The structure of complex **3** in Figure 2 adopts a typical dinuclear metallacyclic structure where each Mn core with its distorted octahedral geometry is bonded to two phenyl selenolato groups. The Mn_2Se_2 ring is almost coplanar and associates with angles of 95.730(13)° for Mn(1)-Se(1)-Mn(2) and 84.132(19)° for Se(1)-Mn(2)-Se(2). The distance between the Mn centers is about 3.75 Å, which probably signifies the absence of a Mn-Mn single bond. The two phenyl rings of the selenolato bridging ligands are in a *cis* conformation. The pyridine ligand is coordinated perpendicular to the Mn_2Se_2 plane with a Mn1-N1 distance of 2.103Å. Because of the asymmetry, each Mn-Se distance varies slightly with the Mn1-Se distances being longer than the Mn2-Se counterparts. The bond lengths of the CO terminal ligands coordinated to Mn1 are also slightly longer than those coordinated to Mn2 due to the stronger electron-donating effects of pyridine.

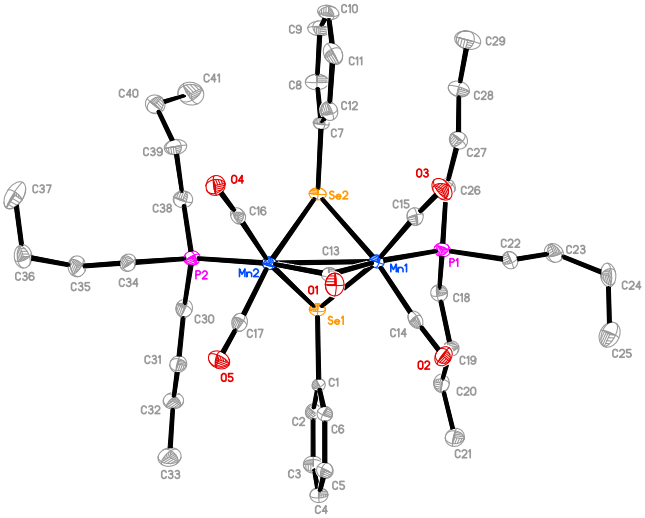

Fig. 1 Displacement ellipsoid plot of solid-state structure **2**. Hydrogen atoms are omitted for clarity. Selected bond lengths (Å) and angles (°): Mn1-Mn2, 2.6528(6); Mn1-Se2, 2.4601(5); Mn1-C13, 2.032(3); Mn1-C14, 1.790(3); Mn1-P1, 2.3021(8); Mn1-Se2-Mn2, 65.185(15); Se2-Mn1-Se1, 74.931(15); Mn2-C13-Mn1, 81.86(11); P2-Mn2-Mn1, 144.19(3). Note that disorder was encountered in the positions of C40 and C41 in one of the n-butyl group.

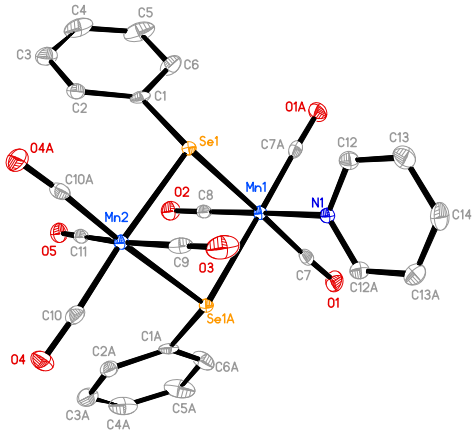

Fig. 2 Displacement ellipsoid plot of solid-state structure **3**. Hydrogen atoms are omitted for clarity. Selected bond lengths (Å) and angles (°): Se1-Mn1, 2.5301(4); Se1-Mn2, 2.5104(4); Mn1-N1, 2.103(3); Mn1 C7,1.793(3); Mn2-Se1-Mn1, 95.730(13); C8-Mn1-N1, 176.44(14).

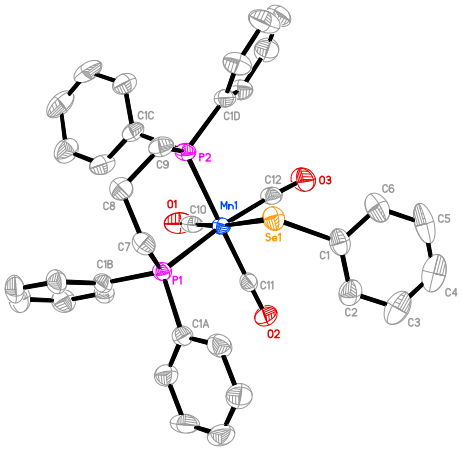

Fig. 3 Displacement ellipsoid plot of solid-state structure **4**. Hydrogen atoms are omitted for clarity. Selected bond lengths (Å) and angles (°): Mn1-Se1, 2.5417(8); Mn1-C10, 1.798(6); Mn1-C11, 1.812(5); Mn1-C12, 1.807(5); Mn1-P1, 2.3536(14); Mn1-P2, 2.3446(14); C10-Mn1-Se1, 172.31(16); C11-Mn1-P2, 176.84(15); P2-Mn1-P1, 90.37(5).

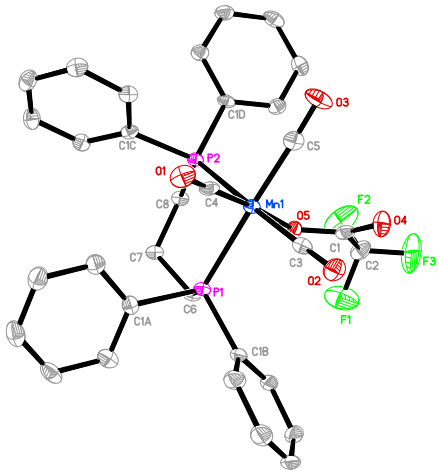

Fig. 4 Displacement ellipsoid plot of solid-state structure **5**. Hydrogen atoms are omitted for clarity. Selected bond lengths (Å) and angles (°): Mn1-O5, 2.055(2); Mn1-C3, 1.834(3); Mn1-C4, 1.782(3); Mn1-C5, 1.835(3); Mn1-P1, 2.3449(12); Mn1-P2, 2.3661(13); C4-Mn1-O5, 176.75(9); C5-Mn1-P1, 174.68(7); P1-Mn1-P2, 89.44(5).

For the structure of **4** in Figure 3, the chelating DPPP ligand forms a boat-like cyclohexane ring with the Mn center. Each of the phosphine atom is trans to a CO ligand with the Mn1-P1 and Mn1-P2 bond distances of 2.3536(14) Å and 2.3446(14) Å respectively. The selenolato ligand is also trans to a CO ligand with the Mn-Se distance of 2.5417(8)Å.

We have also managed to analyse the product (complex **5**) resulting from the addition of CF_3COOH to an acetonitrile solution of **4**. Figure 4 shows the structure of **5** which bears much resemblance to **4** except that the selenolato group has been substituted with a CF_3COO^- ligand with a Mn-O distance of 2.055(2) Å. The trans-orientation of the DPPP ligand with respect to the CO ligands remains similar to that in complex **4**.

Cyclic voltammetry

Cyclic voltammetry (CV) has been used to determine the overpotential for proton reduction catalyzed by the Mn complexes. Due to solubility issues, the CV experiments have been carried out in dichloromethane instead of acetonitrile solvent, with CF_3COOH acting as the proton source and tetrabutylammonium hexafluorophosphate Bu_4NPF_6 as the electrolyte.[20,21] The thermodynamic potential for free CF_3COOH reduction has already been determined to be -0.89V in acetonitrile with respect to the Fc^+/Fc couple (Fc = ferrocene). All potentials quoted henceforth are referenced to the ferrocene couple.

Figure 5 shows the cyclic voltammograms for the dinuclear manganese complexes **1** to **3**. In the absence of acid, a chemically irreversible molecular reduction peak for each of the complexes **1** to **3** was observed at -1.78V, -1.68V and -1.73V in CH_2Cl_2 respectively (Table 1). As all the complexes contain a Mn(I) center, we have assigned the peak to the reduction of

Mn(I) to Mn(0) for the complexes. Remarkably, these molecular reduction peaks appear to occur within a range of only 0.1V despite the difference in the ligands. When CF_3COOH was added to **1**, the molecular peak appeared to increase. As more acid was added, the peak continued to grow in intensity, thus we have assigned this peak to be that of the catalytic proton reduction. In the absence of the manganese complexes, no acid reduction peaks were observed until -2.1V to -2.2V where the acid is believed to be reduced by the electrode itself.

Similarly, the catalytic reduction peaks were observed close to the molecular reduction peaks for complexes **2** and **3**. The catalytic peak positions appear to be stable towards different acid concentrations although it has been reported that the use of certain proton sources such as acetic acid can shift the potentials significantly due to conjugation effects.[14] However very high acid to catalyst ratio may still shift the potential to more negative values, as exemplified in Figure 5a for complex **1**. If the catalytic peak potential is taken to represent the average proton reduction potential, the overpotential with respect to the thermodynamic CF_3COOH reduction (-0.89V) for complexes **1** to **3** can be determined to be 0.89V, 0.79V and 0.84V respectively (Table 1). Although complex **2** gives rise to the lowest overpotential, the values for all three complexes differ only by 0.1V. Meanwhile, if the homoconjugation effect of TFA is considered, the overpotential would become larger while Helm's method would give a slightly larger value.[22] The overpotentials for these Mn complexes lie in the middle of the range of overpotentials (0.3V to 1.2V) measured for the much more extensively-studied diiron dithiolate systems.[10]

Table 1 Comparison of the catalytic potential, the overpotential and the catalytic current of the Mn complexes

	Catalytic peak (V)	Overpotential (V)[a]	Catalytic efficiency.[b]
1	-1.78	0.89	0.5
2	-1.68	0.79	0.2
3	-1.73	0.84	0.4

[a]Overpotential(V)=$E°_{HA/H2} - E_{cat}$, where $E°_{HA/H2}$ is the standard reduction potential of the acid; [b]Catalytic efficiency=$(i_{cat}/i_d)/(c_{HA}/c_{cat})$.[10] i_{cat} is measured for 10 acid equivalent.

In order to further assess the performance of the Mn complexes as proton reduction catalysts, we have also measured the catalytic efficiency at a fixed ratio of acid concentration to the complex concentration. As shown in Table 1, complex **1** appears to be most efficient, followed by **3** and **2**. The catalytic efficiency values are comparable to those generated by the diiron dithiolate systems.[10] The presence of a phosphine or pyridine ligand in **2** and **3** respectively also does not appear to facilitate efficient proton reduction. In fact it appears to be a common observation that the catalytic current tends to be lower when the overpotential for proton reduction is also lower, as exemplified by **2**.[10]

Interestingly, the CV carried out for complex **4** in the absence of acid did not show a reduction peak in the range studied. No obvious peak appeared even when a large acid equivalent was used. We have attributed this observation to the fact that the Mn center in **4** is already electron-rich due to the strong electron-donating properties of the DPPP ligand. The complex is presumably reduced only at much more negative potential. As mentioned, complex **4** can be converted to **5** upon addition of TFA. Complex **5** also did not show any reduction peaks with or without acid addition. A solution of 1mM of the manganese complexes **1**-**3** with excessive amount of CF_3COOH in 0.1M Bu_4NPF_6 in dichloromethane was electrolyzed at -1.80 V vs Fc^+/Fc in a gas-tight electrochemical cell. The average Faraday yield has been determined to be 84±12%.

(a)

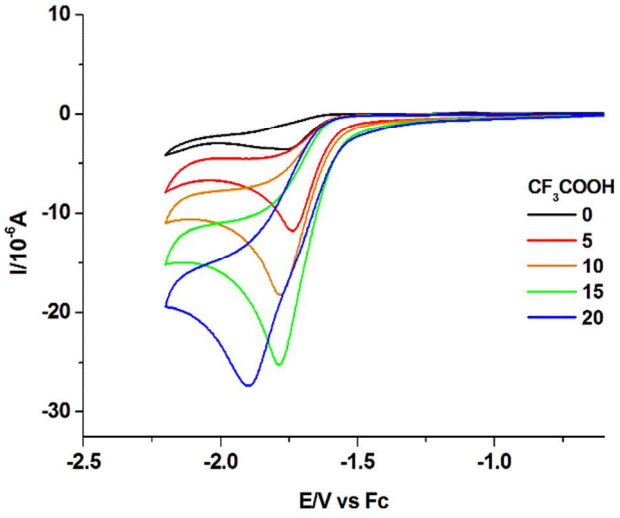

(b)

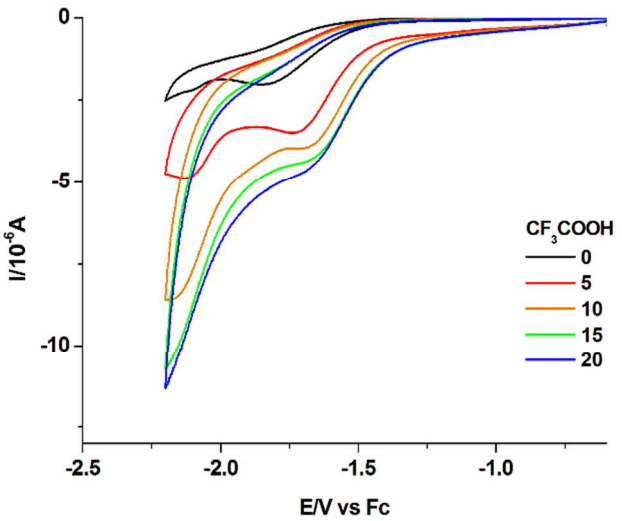

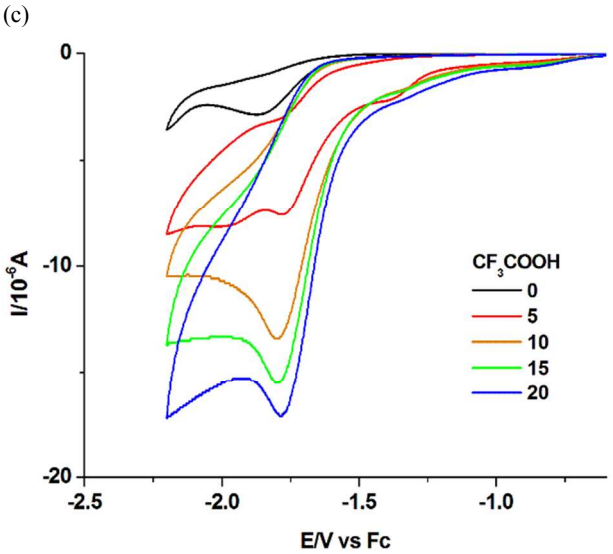

Fig. 5 Cyclic voltammograms of complexes **1**(a), **2**(b), **3**(c) (1.0 mM) in CH_2Cl_2 with 0.1 M Bu_4NPF_6 at 100 mV/sec scan rate, 1mm glassy-carbon working electrode, platinum counter electrode at 295 K with CF_3COOH (0 to 20mM) as the proton source.

Proposed Mechanism

The mechanism for the electroreduction of protons catalyzed by complexes **1** to **3** was next investigated. To ascertain whether the catalysis is initiated by the acid itself, we have reacted the acid with each of the complexes at the concentration ratio used for the CV experiments. However, no spectral changes were observed for the νCO bands of complexes **1** to **3** when the reactions were monitored via FTIR absorption. Only complex **4** reacts with TFA to produce **5**. In addition, we have also reacted complex 1 with sodium in THF in order to simulate the one-electron reduction process. The initial four peaks of 1 disappear gradually and are replaced by three new peaks at 2045, 1973 and 1904 cm^{-1}. The peak pattern bear resemblance to mononuclear Mn(I) complexes of formula $Mn(CO)_3(L_2)(X)$ where the L ligands are trans to each other. Hence we have tentatively assigned the carrier of the peaks to $Mn(CO)_3(THF)_2(SePh)$ complex (See Supporting Information)[23]. Unofrtunately we are unable to detect infrared signals due to any Mn(0) complexes.

In addition, as the catalytic reduction peaks for complexes **1** to **3** appear close to their molecular reduction peaks, we propose that an electrochemical step **E** in the proton reduction pathway is the initiation step. For the subsequent steps, we have based our proposed mechanism on the diiron dithiolate systems to which our manganese complexes bear much structural resemblance in terms of the dimetallic nature and the use of thiolates or its selenium counterparts as bridging ligands.[24]

Scheme 3 shows two possible electrochemical pathways, arising from the reduction of the Mn complexes as starting points. The dimeric Mn complexes representing **1**, **2** and **3** are shown as examples here. Either the ECCE (electrochemical–chemical–chemical–electrochemical) or EC process is consistent with the cyclic voltammetry data. In the former mechanism, one of the Mn(I) centers is reduced to Mn(0) followed by a proton capture to give an Mn-H bond. The Mn center at this stage may be regarded as an Mn(II) state coordinated to a hydride (H^-). This manganese hydride intermediate reacts with a second proton to generate a Mn(II)-Mn(I) cation carrying a dihydrogen unit. The catalytic cycle is completed upon a second reduction and concomitant release of H_2.

The alternative EC process involves the same manganese hydride intermediate as in the ECEC process. A bimolecular reaction has to occur between two of these sterically-bulky Mn intermediate to produce dihydrogen and restore the catalytic cycle. However the concentrations of the intermediates are expected to be low and hence reduce the likelihood of reaction for both the electron transfer and the proton acceptor steps.

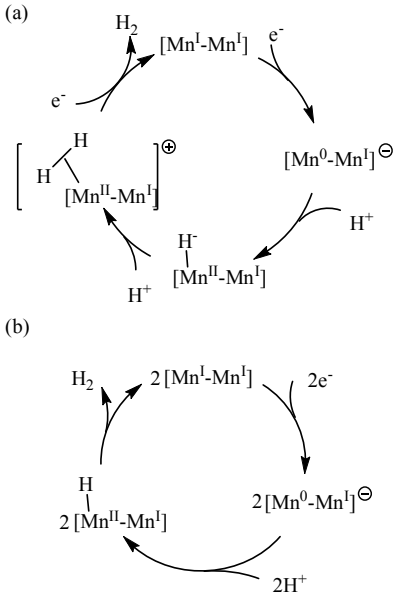

Scheme 3. Proposed mechanism for proton reduction catalyzed by dinuclear manganese complexes: (a) ECCE (b)EC.

Conclusions

Four manganese selenolato carbonyl complexes have been synthesized and characterized by X-ray crystallography. Their electrocatalytic proton reduction properties were measured with CF_3COOH as the proton source in CH_2Cl_2. Similar overpotentials ranging from 0.79V to 0.89V were determined for these complexes. The presence of different ligands such as phosphine and pyridine on some of the complexes only made moderate differences on the overpotential and efficiency of the proton reduction process. Reactivity studies and cyclic voltammetry data suggest that the first step in the proton reduction pathway occurs via electroreduction of the Mn complexes.

Experimental methods

General Procedures. All reactions were carried out under reduced pressure using standard vacuum line and Schlenk techniques unless otherwise stated. Photochemical reactions were performed using Legrand broadband ultraviolet lamp (200W, 200-800 nm). ^{1}H NMR spectra was recorded using Bruker ACF300 NMR spectrometer at room temperature. FTIR absorption spectra were recorded on a Shimadzu IR-Prestige 21 spectrometer. Single crystal X-ray structural studies were performed on Bruker-AXS Smart Apex CCD Single-Crystal Diffactometers. Data were collected at 100(2)K using graphite monochromated Mo Kα radiation (=0.71073Å). Data collection was evaluated using SMART CCD system.

Electrochemical Experiments. Cyclic voltammetry experiments were conducted with a computer-controlled potentiostat using a three electrode system. Working electrodes were 1 mm diameter planar glassy carbon disks, used in conjunction with a platinum auxiliary/counter electrode and a silver wire miniature reference electrode connected to the test solution via a salt bridge (containing 0.5 mol dm^{-3} Bu_4NPF_6 in CH_2Cl_2). Prior to each scan, the solutions used for voltammetric analysis were de-oxygenated by purging with high purity Ar gas, and the working electrodes were prepared by polishing with alumina oxide (grain size 0.3 micrometer) slurry on a Buehler Ultra-pad polishing cloth, rinsing with ultrapure water, acetone, and then drying with a tissue. Accurate potentials were obtained by using ferrocene (Fc) as an internal standard, which was added to the test solution at the end of the measurements. All voltammetric experiments were conducted in a Faraday cage at 295 (±2) K. The test solutions were comprised of 1 mM of analyte and 0.1 M of the supporting electrolyte, tetrabutylammonium hexafluorophosphate (Bu_4NPF_6), in CH_2Cl_2.

(b) Controlled Potential Electrolysis. A solution of 1mM of the manganese complexes with 50 mM CF_3COOH in 0.1M Bu_4NPF_6 in dichloromethane was electrolyzed at -1.80 V vs Fc^+/Fc in a gas-tight electrochemical cell. The experiment was carried out three times, with the current and electrolysis period monitored. The average values were calculated. The gaseous content of the reaction vessel was removed with a syringe of 1 cm^3 volume and injected into a mass spectrometer which has been tuned to monitor signals at m/z = 2, corresponding to the production of H_2. The signal intensity is calibrated with the signal produced by the injection of a known pressure of H_2 gas taken from a H_2 cylinder (Soxal, 99.99%). The Faraday yield of 84±12% was determined by the average of three readings of [H_2 detected]/[electrons used for electrolysis] ratios.

Synthesis of $Mn_2(CO)_8(\mu\text{-}SePh)_2$ (1). The synthesis of complex **1** has already been described in reference 19.

Synthesis of $Mn_2(CO)_4(\mu\text{-}CO)(\mu\text{-}SePh)_2(L)_2$ (2, L=PBu_3, Tri-n-butylphosphine). $Mn_2(CO)_8(\mu\text{-}SePh)_2$ (32.3 mg, 0.05 mmol) and Tri-n-butylphosphine (20.2 mg, 0.10 mmol) were added to a 25mL of hexane and subjected to photolysis for 15 mins. Suitable crystal of 2 was grown by dissolving them in dichloromethane/hexane and stored at low temperature for days. Yield: 31 mg, 64.0%. Anal. Calc. for $C_{41}H_{64}Mn_2O_5P_2Se_2$: C, 50.94; H, 6.67. Found: C, 51.22; H, 7.05. IR νCO (CH_2Cl_2): 1904(s), 1945(s), 2010(vs). ^{1}H NMR δ($CDCl_3$): 0.73(t,10H,-CH_3), 0.96-1.90(m,18H, -P(CH_2)$_3$). 7.13-7.38 (m, 10H,-Ph).

Synthesis of $Mn(CO)_4(\mu\text{-}SePh)_2Mn(CO)_3(Py)$ (3, Py=pyridine). $Mn_2(CO)_{10}$ (100 mg, 0.26 mmol) , diphenyl diselenide (163 mg, 0.52 mmol) and pyridine (82 mg, 1.04 mmol) were added to a 50mL of hexane and subjected to photolysis for 3 h. Suitable crystals of **3** were grown by dissolving them in dichloromethane/hexane and stored at low temperature for days. Yield: 107 mg, 58.5% (based on $Mn_2(CO)_{10}$). Anal. Calc. for $C_{24}H_{15}Mn_2NO_7Se_2$: C, 41.35; H, 2.17. Found: C, 41.62 ; H, 2.26.

IR νCO (CH_2Cl_2): 1912(s), 1934(s), 2001(s), 2020(vs). ^{1}H NMR δ ($CDCl_3$): 7.29-7.59 (m, 10H, from Ph, 5H, pyridine).

Synthesis of $Mn(CO)_3(SePh)$ (DPPP) (4, DPPP=1,3-bis(diphenylphosphino)propane). $Mn_2(CO)_{10}$ (100 mg, 0.26 mmol) , diphenyl diselenide (163 mg, 0.52 mmol) and 1,3-Bis(diphenylphosphino)propane(219mg, 0.52mmol) were added to a 50mL of hexane and subjected to photolysis for 3 h. Suitable crystals of **4** were grown by dissolving them in dichloromethane and stored at room temperature for days. Yield: 193mg, 52.4% (based on $Mn_2(CO)_{10}$). Anal. Calc. for $C_{36}H_{31}MnO_3P_2Se$: C, 61.12; H, 4.42. Found: C, 61.45; H, 4.50. IR νCO (CH_2Cl_2): 1904(s), 1945(s), 2010(vs). ^{1}H NMR δ($CDCl_3$): 1.50-2.80 (m, 6H, CH_2), 6.78-7.72 (m, 15H, -Ph);

Synthesis of $Mn(CO)_3(O_2CCF_3)$(DPPP) (5). 50 mg $Mn(CO)_3$(SePh) (DPPP) was dissolved in CH_2Cl_2 and equivalent CF_3COOH was added to generate **5**. Suitable crystal of complexes 3 was grown by dissolving them in dichloromethane and stored at room temperature for days. Yield: 45mg, 89.5%. Anal. Calc. for $C_{32}H_{26}F_3MnO_5P_2$: C, 57.85; H, 3.94. Found: C, 58.03; H, 4.15. IR νCO (CH_2Cl_2): 1918(s), 1967(s), 2035(vs). ^{1}H NMR δ ($CDCl_3$): 1.31-2.71(m, 6H,CH_2). 7.31-7.43 (m, 10H, -Ph).

Acknowledgements
This work was supported by a NUS research grant (143-000-553-112).

Notes and references
[a] Department of Chemistry, National University of Singapore, 3 Science Drive 3, Singapore 117543.
[b] Division of Chemistry & Biological Chemistry, School of Physical and Mathematical Sciences, Nanyang Technological University, 21 Nanyang Link, Singapore 637371
†Electronic Supplementary Information (ESI) available: See DOI: 10.1039/b000000x/

(1) S. U. M. Khan, M. Al-Shahry, W. B. Ingler, *Science*., 2002, **297**, 2243-2245.
(2) N. S. Lewis, D. G. Nocera, *Proc. Natl. Acad. Sci. U. S. A*., 2006, **103**, 15729-15735.
(3) H. B. Gray, *Nat. Chem*., 2009, **1**, 7.
(4) R. Eisenberg, *Science*., 2009, **324**, 44-45.

(5) (a) C. Tard, C .J. Pickett, *Chem. Rev.,* 2009, **109**, 2245-2274; (b) J. Fritsch, P. Scheerer, S. Frielingsdorf, S. Kroschinsky, B. Friedrich, O. Lenz, C. M. Spahn, C. M., *Nature*, 2011, **479**, 249-252.

(6) Y. Higuchi, H. Ogata, K. Miki, N. Yasuoka, T. Yagi, *Structure.,* 1999, **7**, 549-556.

(7) E. Garcin, X. Vernede, E. C. Hatchikian, A. Volbeda, M. Frey, J. C. Fontecilla-Camps, *Structure.,* 1999, **7**, 557-566.

(8) (a) Z. Li, Z., Y. Ohki, K. Tatsumi, K., *J. Am. Chem. Soc*., 2005, **127**, 8950-8951; (b) S. Ogo, K. Ichikawa, T. Kishima, T. Matsumoto, H. Nakai, K. Kusaka, T. Ohhara, *Science*, 2013, **339**, 682-684.

(9) (a) L. C. Sun, B. Akermark, S. Ott, *Coord. Chem. Rev*., 2005, **249**, 1653-1663. (b) A. Parkin, G. Goldet, C. Cavazza, J. C. Fontecilla-Camps, F. A. Armstrong, *J. Am. Chem. Soc.,* 2008, **130**, 13410-13416; (c) F. Gloaguen, T. B. Rauchfuss, *Chem. Soc. Rev*., 2009, **38**, 100-108; (d) A. C. Marr, D. J. E. Spencer, M. Schröder, *Coord. Chem. Rev.,* 2001, **219**, 1055-1074; (e) M. Y. Darensbourg, E. J. Lyon, J. J. Smee, *Coord. Chem. Rev*., 2000, **206**, 533-561.

(10) (a) L. C. Song, *Acc. Chem. Res.*, 2005, **38**, 21-28;(b) G. A. N. Felton, C. A. Mebi, B. J. Petro, A. K. Vannucci, D. H. Evans, R. S. Glass, D. L. Lichtenberger, *J. Organomet. Chem.,* 2009, **694**, 2681-2699.

(11) M. Wang, L. Chen, L. Sun, *Energy Environ. Sci.,* 2012,***5,*** 6763-6778.

(12) S. Ott, M. Kritikos, B. Åkermark, L. Sun, R. Lomoth, *Angew. Chem. Int. Ed.,* 2004, **116**, 1024-1027.

(13) L.C. Song, J. P. Li, Z. J. Xie, H. B. Song, *Inorg. Chem.*, 2013, **52**, 11618-11626.

(14) M. K. Harb, U. P. Apfel, J. Kübel, H. Görls, G. A. N. Felton, T. Sakamoto, D. H. Evans, R. S. Glass, D. L. Lichtenberger, M. El-Khateeb, *Organometallics.,* 2009, **28**, 6666-6675.

(15) M. K. Harb, T. Niksch, J. Windhager, H. Görls, R. Holze, L. T. Lockett, N. Okumura, D. H. Evans, R. S. Glass, D. L. Lichtenberger, *Organometallics.,* 2009, **28**, 1039-1048.

(16) C. Wombwell, E. Reisner, *Dalton. Trans.,* 2014, **43**, 44834493.

(17) K. Hou, K. H. T. Poh, W. Y. Fan, *Chem. Comm.*, 2014, **50**, 6630-6632.

(18) K. Hou, W. Y. Fan, *Dalton. Trans*, 2014, **43**, 16977-16980.

(19) E. W. Abel, B. C. Crosse, G. V. Hutson, *J. Chem. Soc. A.,* 1967, 2014-2017.

(20) M. J. Rose, H. B. Gray, J. R. Winkler, *J. Am. Chem. Soc.,* 2012, **134**, 8310-8313.

(21) L. C. Song, J. P. Li, Z. J. Xie, H. B. Song, *Inorg. Chem.,* 2013, **52**, 11618-11626.

(22) (a) Fourmond, V.; Jacques, P.-A.; Fontecave, M.; Artero, V. Inorg Chem., 2010, 49, 10338-10347; (b) Appel, A. M.; Helm, M. L. ACS Catal. 2014, 4, 630-633.

(23) M. A. Beckett, D. S. Brassington, S. J. Coles, T. Gelbrich, M. E. Light, M.B . Hursthouse, *J. Organomet.Chem*., 2003, **688**, 174-180.

(24) D. Chong, I. P. Georgakaki, R. Mejia-Rodriguez, J. Sanabria-Chinchilla, M. P. Soriaga, M. Y. Darensbourg, *Dalton. Trans.*, 2003, 4158-4163.